

μ SR study of the intermediate heavy-fermion system CeRuSi₂

V. N. Duginov, V. G. Grebinnik, K. I. Gritsaj, T. N. Mamedov, V. G. Olshevsky, V. Yu. Pomjakushin, and V. A. Zhukov
Joint Institute for Nuclear Research, Dubna 141980, Russia

I. A. Krivosheev and A. N. Ponomarev
Kurchatov Institute, Kurchatov square 1, Moscow 123182, Russia

V. N. Nikiforov* and Yu. D. Seropegin
Faculty of Physics, Moscow State University, Moscow 119899, Russia

M. Baran and H. Szymczak
Institute of Physics, Polish Academy of Science, 02-668 Warszawa, Poland
(Received 18 April 1996)

Zero-field (ZF), longitudinal field (LF), muon spin relaxation (μ SR), and transverse field (TF) muon spin rotation (μ SR) measurements have been carried out on a polycrystalline sample CeRuSi₂. ZF data show a sharp increase in the muon relaxation rate below the temperature 12 K ($0.42 \mu\text{s}^{-1}$ at $T=4.2$ K), justifying the transition to the magnetically ordered state. From the LF measurements at $T=4.2$ K, we found that the magnetic fields on the muon, B_μ , produced by the cerium magnetic moments are mainly static: The external longitudinal field of 150 G practically recovers muon spin polarization. In the paramagnetic phase the polarization has an exponential form in the whole range of temperatures $20 \text{ K} < T < 300 \text{ K}$, but LF experiments at $T=20$ K show that there is a static contribution ($\sim 70\%$). This situation is discussed within the framework of the double-relaxation model. Hysteresis in (B - H) observed in the TF experiment and the results of magnetization measurements agree with ferromagneticlike ordering below $T_c=11.6$ K. The width of the field distribution obtained in the TF experiment corresponds to the ordered moment (0.005 – 0.05) μ_B , depending on the assumed muon site. [S0163-1829(97)02617-9]

I. INTRODUCTION

The CeTX₂ series of cerium ternary intermetallic compounds, where T is a transition metal and X denotes Si, Ge, and Sn, exhibits interesting properties, such as heavy-fermion or Kondo-lattice¹ behavior [CePtSi₂ with the electronic specific heat coefficient $\gamma=1700$ mJ/mol K² (Ref. 2)], mixed valence,³ and spin-fluctuating behavior observed in CeNiSi₂ (Ref. 4) and CeRhSi₂.⁵ A recent report on CeRuSi₂ (Ref. 6) has shown that this compound crystallizes into a structure which is different from the CeNiSi₂ type common for other compounds of this series and has the NdRuSi₂-type monoclinic crystal structure of the $P2_1/m$ space group. The temperature dependence of resistivity $R(T)$ has a sharp rapid decrease below $T_1 \sim 11$ K.⁶ The temperature dependence of the magnetic susceptibility $\chi(T)$ can be described by the Curie-Weiss law at temperatures $60 \text{ K} < T < 300 \text{ K}$ with Curie constant $C=1.22 \times 10^{-4}$ emu/g Oe. The effective moment deduced from the Curie constant was found to be $\mu_{\text{eff}} \approx 1.7 \mu_B$,⁶ which is sufficiently smaller in comparison with that of the free Ce³⁺ ion and those found for other Ce-based heavy-fermion (HF) compounds. A sharp upturn in the $\chi(T)$ curve, spontaneous magnetic moment, and hysteresis of the field dependence of magnetization was observed below T_1 . The low-temperature electronic specific heat coefficient $\gamma \sim 100$ mJ/mol K² is markedly enhanced and a sharp λ -shaped anomaly confirms the presence of a magnetic transition at T_1 . The data obtained^{6,7} allow one to conclude that CeRuSi₂ with the NdRuSi₂-type crystal structure (new for the CeTX₂

series) might belong to a relatively rare family of compounds where the Kondo effect and ferromagnetism (or a more complicated magnetic order) coexist.⁸

The aim of the present work is to provide more information on the magnetic properties of CeRuSi₂ from muon spin relaxation (μ SR) measurements. The μ SR method⁹ is extremely sensitive to both static magnetic order (up to $0.001 \mu_B$) and spin dynamics (10^5 – 10^{10} Hz) and is widely used in investigation of the HF system.¹⁰

II. EXPERIMENT

The sample was synthesized by a method described elsewhere.⁷ The x-ray phase analysis (resolution was better than 5%) and x-ray microanalysis (with a resolution of 2–3 %) did not detect any traces of extrinsic phases. X-ray analyses were performed with a DRON-2.0 (Fe $K\alpha$ radiation) device using Cu $K\alpha$ and Cu $K\alpha$ lines and germanium as the internal reference. The observed reflections were identified by comparing the patterns with the ASTM catalog. A "Camebax" microanalyzer was employed to perform local x-ray spectral analyses of the sample using titanium $K\alpha$, germanium $K\alpha$, and niobium $L\alpha$ lines. The x-ray investigations show that the crystal structure of the CeRuSi₂ compound is of the NdRuSi₂ type. The density calculated from the x-ray data is approximately 9.485 g/cm³, and the lattice parameters are found to be $a=4.478(1)$ Å, $b=4.093(1)$ Å, $c=8.302(5)$ Å, and $\beta=102.53(3)$.

The present μ SR measurements were performed on the

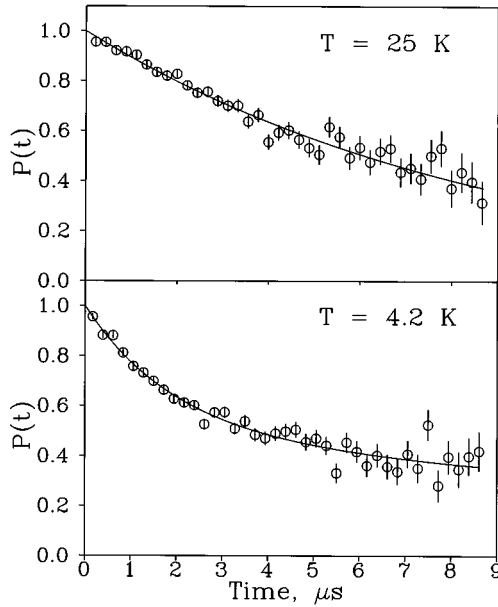


FIG. 1. Time dependence of muon spin polarization (ZF) at $T=4.2$ and 25 K. Solid lines show the fit to Eqs. (1) and (2), respectively.

muon channel of the LNP JINR phasotron using the spectrometer MUSPIN.¹¹ The sample used in the μ SR experiment consisted of a large number of polycrystalline pieces with typical size 3 mm, packed in a paper container in the form of a cylinder with dimensions 30×5 mm². The cylinder axis was directed along the initial muon polarization. The sample was mounted in a He/N₂ flow cryostat. The temperature was stabilized to better than 0.1 K. Magnetization measurements were carried out with the superconducting quantum interference device (SQUID) magnetometer (Quantum Design, MPMS-5) at low temperatures in a magnetic field up to 50 kG.

III. RESULTS

Zero-field (ZF) μ SR measurements were performed in the temperature interval 4.2 K $< T < 300$ K above and below the Curie temperature. In both regions the muon spin polarization function $P(t)$ has a nonoscillating form (Fig. 1). In the paramagnetic region 20 K $< T < 300$ K, the polarization func-

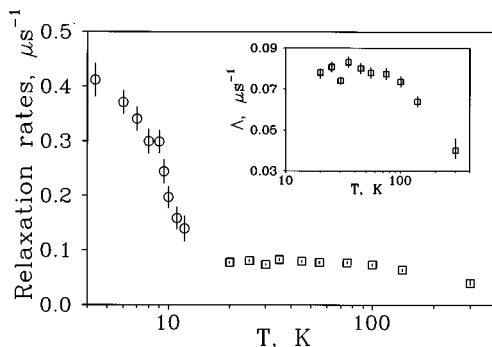


FIG. 2. Relaxation rates vs temperature: squares (see also inset) are Λ above T_C [Eq. (1)] and circles are Λ_{fast} below T_C [Eq. (2)].

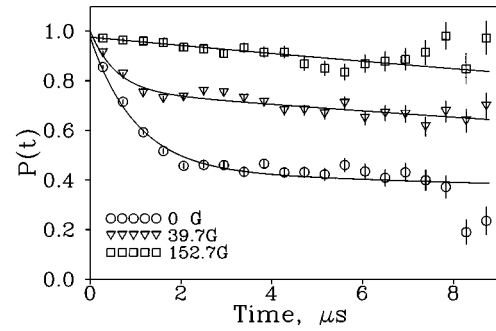


FIG. 3. Examples of the muon spin polarization function obtained in the LF experiment ($T=4.2$ K). Solid lines are the fit to Eq. (3).

tion is well fitted by a single exponent function

$$P(t) = P(0) \exp(-\Lambda t). \quad (1)$$

$P(0)$ was determined in TF experiment at $T \gg T_C$. Below the Curie temperature T_C , the relaxation function consists of two parts: a fast- and a slow-relaxing component, and reasonable fit was obtained using the formula

$$P(t) = P(0) \left[\frac{2}{3} \exp(-\Lambda_{\text{fast}} t) + \frac{1}{3} \exp(-\Lambda_{\text{slow}} t) \right]. \quad (2)$$

This function is usual for a polycrystalline sample when the magnetic field distribution on the muon is isotropic. One-third of the static internal magnetic fields, directed along the initial muon spin polarization, does not depolarize the muon spin. Figure 2 presents temperature dependences of relaxation rates: Squares are Λ above T_C [Eq. (1)] and circles are Λ_{fast} below T_C [Eq. (2)]. The inset shows Λ in the paramagnetic phase. The relaxation rate of the slow-relaxing component Λ_{slow} [Eq. (2)] does not exceed the value of the relaxation rate in the paramagnetic region.

Longitudinal field (LF) measurements were performed below T_C (at $T=4.2$ K) and above T_C (at $T=20$ K) in order to probe the dynamics of the magnetic field. Several examples of experimental polarization are presented in Fig. 3. One can see that the longitudinal field of 150 G practically recovers fast depolarization of the muon spin. At the same time a small nonzero residual value $\Lambda \sim 0.030(5) \mu\text{s}^{-1}$ exists even in the field of 400 G. The LF experiment above T_C (at $T=20$ K) also shows the residual depolarization $\Lambda \sim 0.025(5) \mu\text{s}^{-1}$ (up to 4.2 kG). At 20 K we obtain this value even in the first

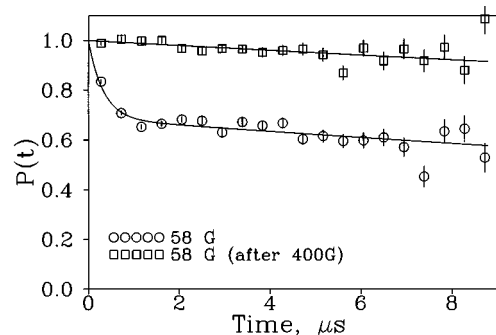


FIG. 4. Muon spin polarization functions measured in the longitudinal field of 58 G in an ascending and descending (after LF = 400 G) field scan ($T=4.2$ K).

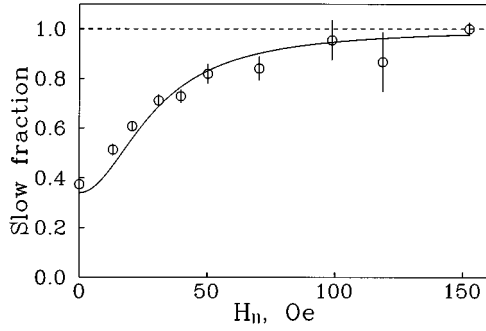


FIG. 5. a_{slow} [Eq. (3)] vs the longitudinal field ($T=4.2$ K). The solid line is a guide to the eye.

nonzero measured longitudinal field (~ 85 G). Below T_C we found hysteresislike behavior of the relaxation rate. Figure 4 shows muon spin polarization functions measured in a longitudinal field of 58 G in an ascending and descending field scan. The recovery of the amplitude of a slow-relaxing component versus the longitudinal field is presented in Fig. 5. The fit was obtained using the formula,

$$P(t) = P(0)[a_{\text{fast}}\exp(-\Lambda_{\text{fast}}t) + a_{\text{slow}}\exp(-\Lambda_{\text{slow}}t)]. \quad (3)$$

TF measurements were performed at $T=4.2$ and 20 K. Figure 6 presents the field dependence of $(B-H)$ and relaxation rates at $T=4.2$ K [zero-field cooled (ZFC)] and $T=20$ K. One can see the hysteresis in the $(B-H)$ versus transverse external field dependence. We do not insist on the absolute value of $(B-H)$ due to the problem of the precise determination of the external field near the sample. Error bars for $(B-$

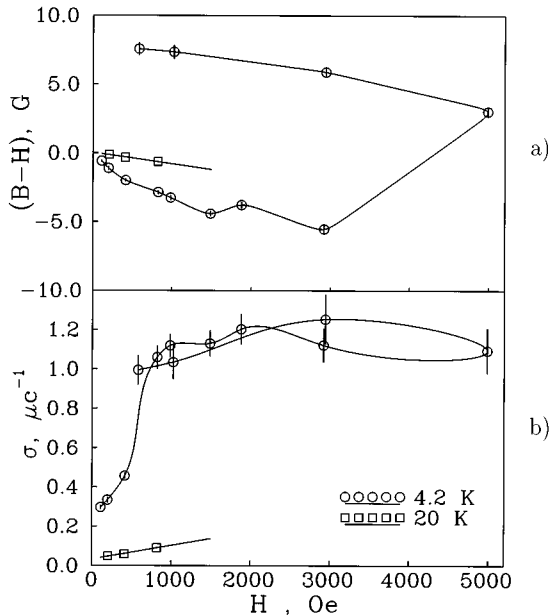


FIG. 6. (a) $(B-H)$ [the error bars present only statistical errors (see the text)] and (b) the exponential relaxation rate vs the transverse external field (ZFC). Circles and squares are the data at $T=4.2$ and 20 K, respectively. The solid line is a guide to the eye.

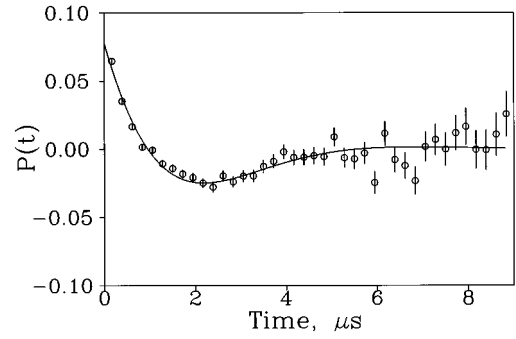


FIG. 7. Experimental polarization ($T=4.2$ K) after switching off the transversal field (5 kG). The solid line is the fit to Eq. (4).

$H)$ in Fig. 6(a) show only statistical errors. The demagnetization factor is not included in the data in the figure either. In the ordered phase ($T=4.2$ K), the $\Lambda(H)$ slope is much steeper than above the Curie temperature ($T=20$ K), indicating magnetization of the ferromagnetic sample. The relaxation rate in the field ~ 100 G (ZFC) equals $0.3 \mu\text{s}^{-1}$, but at the same temperature and field in the field cooling experiment (100 G) it was found to be $0.54 \mu\text{s}^{-1}$.

After switching off the transverse field of 5 kG at $T=4.2$ K, the polarization function has a typical static form (Fig. 7). But this form is not simple, and a reasonable fit was obtained only for the function

$$P(0)\{a_1\exp(-\Lambda t)\cos(\omega t + \phi) + a_2[1/3 + 2/3(1 - \lambda t)\exp(-\lambda t)]\}, \quad (4)$$

with $\lambda=2.5 \mu\text{s}^{-1}$ and $\omega=1.1 \text{ rad}/\mu\text{s}$.

Figure 8 presents the field dependence of magnetization at different temperatures.

IV. DISCUSSION

In the paramagnetic region we have to take into account two different features of polarization. The first one is that the exponential time dependence of polarization is clear evi-

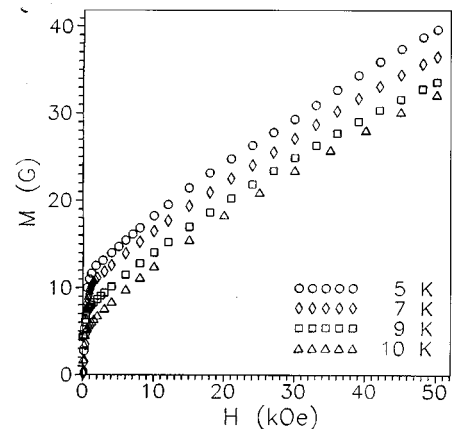


FIG. 8. Field dependence of magnetization at different temperatures. $M=40$ G corresponds to $0.21\mu_B/\text{Ce}$.

dence for the dynamical origin of muon spin relaxation. The existence of this contribution can also be deduced from the residual depolarization $0.025 \mu\text{s}^{-1}$ in LF measurements at $T=20$ K. As we did not see the static picture even at 20 K, we think this dynamics to be due to the fluctuating Ce moments, and it cannot be attributed to some diffusion features (at temperatures $T \leq 100$ K). In the paramagnetic state the main contributions to the Ce moment fluctuations are RKKY and/or dipole interactions and Korringa scattering of the conduction electron (we do not consider slowing down at temperatures $T \geq 20$ K). However, the Korringa mechanism makes the temperature-dependent contribution proportional to T^{-1} . So we can conclude from the data given in Fig. 2 that this contribution is small. A small decrease in the relaxation with increasing temperature at $T \sim 100$ K (Fig. 2) probably originates from the beginning of muon diffusion. From the absence of a LF dependence (at $T=20$ K), we can evaluate the fluctuation frequency by the formula

$$\Lambda \sim \left[1 + \left(\frac{\nu_{\text{LF}}}{\nu} \right)^2 \right]^{-1},$$

where $\nu_{\text{LF}} = \gamma/2\pi\mu$. Here H_{LF} as $\nu \gg 6 \times 10^7$ Hz. The second feature of polarization is the decoupling of muon spin from the nuclear field in LF experiments. Thus the relaxation above the Curie temperature in CeRuSi_2 is due to the static nuclear dipolar moments and fast-fluctuating Ce electronic moments. The phenomenological form of polarization in this case is the product of the exponent and the static Kubo-Toyabe function, which is different from our data. A possible explanation may be found in the fact that Ce moments couple not only muons, but also nuclear moments (the so-called double-relaxation model).¹² In this case we should replace the static Kubo-Toyabe function in relaxation by the dynamic Kubo-Toyabe function $G^{\text{KT}}(\Delta_N, \nu_N^{\text{eff}}, t)$, where $\nu_N^{\text{eff}} = 2\Delta_{\text{NCe}}^2/\nu_{\text{Ce}}$, and Δ_{NCe} is the rms field component at the nuclear due to the Ce electronic moments.¹² So, if $\nu_N^{\text{eff}} \gg \Delta_N$, we get clear exponential relaxation:

$$P \sim \exp \left[- \left(\frac{2\Delta_{\text{Ce}}^2}{\nu_{\text{Ce}}} + \frac{2\Delta_N^2}{\nu^{\text{eff}}} \right) t \right]. \quad (5)$$

Following the above assumption, we can attribute the residual relaxation in LF experiments, $0.025 \mu\text{s}^{-1}$, to the first term in Eq. (5) ($\nu^{\text{Ce}} \gg \nu^{\text{eff}}$).

A sharp increase in the relaxation rate (Fig. 2) below 12 K unambiguously shows that this relaxation is due to the electron moments. In the static limit this relaxation ($0.42 \mu\text{s}^{-1}$ at $T=4.2$ K) corresponds to the rms magnetic field on the muon Δ of the order of 5 G. The lack of precession below T_C indicates that $\langle B \rangle \leq \Delta$.

LF measurements give evidence (Figs. 3, 4, and 5) that the magnetic field distribution is close to the static limit (at the time scale $t \leq 10 \mu\text{s}$ defined by the muon lifetime). The residual relaxation $\Lambda \sim 0.030(5) \mu\text{s}^{-1}$ in a high longitudinal field ($H_{\text{LF}} \gg \Delta_{\text{ZF}} = 5$ G) implies the presence of some dynamics. It is because of this small dynamics that the experimental

polarization $P(t)$ has neither an oscillation form nor a typical minimum expected in the case of a pure static field distribution.

The relaxation rate in TF experiments reflects the anisotropic part of the magnetic field on the muon, which depends on mutual orientation of the external field and crystallographic axes. One of the main contributions comes from the dipole fields. When a polycrystalline sample is magnetized, the anisotropy of the dipole fields broadens the magnetic field distribution on the muon. The relaxation rate is minimal in the fully demagnetized state of the sample below T_C . Magnetization in domains has a tendency to be directed along easy axes, and thus the dipole fields on the muons in different crystallites are close. The external field magnetizes the sample which actually leads to an isotropic (if there is no texture in the sample) distribution of magnetization over the crystallographic axes and, hence, to the increasing magnetic field inhomogeneity. One can see [Fig. 6(b)] that below the Curie temperature the relaxation reaches its maximum at $H \sim 1$ kG, which means that at this field the sample is fully magnetized. This field value coincides with the beginning of the slope change in the magnetization curve (Fig. 8), but differs dramatically from the LF results, where we found practically full recovery of polarization at $H_{\text{LF}} \sim 150$ G (Fig. 5). On the other hand, one can see the increase of magnetization (Fig. 8) above 1 kG with a relatively large slope of the order of $2.75 \times 10^{-3} \mu_B/\text{kG}$. This increase cannot be connected with increasing of the Ce local moments. Indeed, when the sample is fully magnetized, the main contribution in the muon spin relaxation is dipole broadening, which is proportional to the value of the Ce moments. Such a large slope does not correspond to TF μSR [Fig. 6(b)]. Thus we can conclude that the linear increase in magnetization above 1 kG is connected with polarization of conduction electrons, which does not contribute to the muon spin relaxation rate.

The lack of information about the muon site and type of magnetic ordering in this compound does not allow precise determination of the ordered moment. But if we take into account a wide distribution of the magnetic field in this compound, we can approximately estimate the ordered magnetic moment to be $(0.005-0.05)\mu_B$. One can see from Fig. 8 that the saturation moment extrapolated to zero magnetic field ($T=0$) agrees with above estimation.

In summary, our results agree with ferromagnetic like ordering of CeRuSi_2 below 12 K. From the LF measurements ($T=4.2$ K), we found that the magnetic fields on the muon, B_μ , produced by the cerium magnetic moments are mainly static. The width of the field distribution obtained in TF experiments corresponds to the ordered moment $(0.005-0.05)\mu_B$, depending on the assumed muon site. The presence of muon spin relaxation in high longitudinal fields below and above T_C indicates the existence of cerium moment fluctuations. The exponential form of spectra above T_C and decoupling of the muon from the static nuclear moment in LF experiments at the same time may be understood in terms of the double-relaxation model.¹²

ACKNOWLEDGMENTS

The work was supported in part by Grant No. 95-02-04340 of the Russian Foundation for Basic Research.

- * Author to whom correspondence should be addressed at Low Temperature Department, Faculty of Physics, Moscow State University 119899 Moscow, Russia. Electronic address: nvn@lt.phys.msu.su
- ¹N. Grewe and F. Steglich, in *Handbook on the Physics and Chemistry of Rare Earths*, edited by K. A. Gschneider, Jr. and L. Eyring (North-Holland, Amsterdam, 1991), Vol. 14, p. 343.
- ²W. N. Lee, K. S. Kwan, P. Klavis, and R. N. Shelton, *Phys. Rev. B* **42**, 6542 (1990).
- ³J. M. Robinson, *Phys. Rep.* **51**, 1 (1979).
- ⁴V. K. Pecharsky, K. A. Gschneider, and L. Miller, *Phys. Rev. B* **43**, 10 906 (1991).
- ⁵D. T. Androja and B. D. Rainford, *J. Magn. Magn. Mater.* **119**, 54 (1993).
- ⁶A. A. Velikhovski, V. N. Nikiforov, J. Mirkovic, V. Kovacic, M. Baran, and H. Szymczak, *IEEE Trans. Magn.* **MAG-30**, 1208 (1994).
- ⁷V. N. Nikiforov, V. Kovacic, I. O. Grishenko, A. A. Velikhovski, J. Mirkovic, B. I. Shapiev, O. I. Bodak, and Yu. D. Seropegin, *Physica B* **186–188**, 514 (1993).
- ⁸V. Yu. Irkhin and M. I. Katsnelson, *Z. Phys. B* **82**, 77 (1991).
- ⁹A. Schenck, *Muon Spin Rotation Spectroscopy* (Hilger, Bristol, 1985).
- ¹⁰A. Schenck, in *Frontiers in Solid State Sciences*, edited by L. C. Gupta and M. S. Multani (World Scientific, Singapore, 1993), Vol. 2, p. 269.
- ¹¹V. N. Dodokhov, V. N. Duginov, I. A. Gaganov, V. G. Grebinik, S. Kapusta, A. B. Lazarev, V. G. Olshevsky, V. Yu. Pomjakushin, V. S. Roganov, S. N. Shilov, V. A. Zhukov, V. G. Zinov, I. I. Gurevich, B. F. Kirillov, E. P. Krasnoperov, B. A. Nikolsky, A. V. Pirogov, A. N. Ponomarev, V. G. Storchak, V. A. Suetin, S. Safrata, and J. Sebek, *Hyperfine Interact.* **65**, 1167 (1990).
- ¹²D. R. Noakes, J. H. Brewer, D. R. Harshman, E. J. Ansaldo, and C. Y. Huang, *Phys. Rev. B* **35**, 6597 (1987).